Galactose Oxidase Models: Tuning the Properties of Cu^{II} – Phenoxyl Radicals

Aurélie Philibert,[a] Fabrice Thomas,*[a] Christian Philouze,[a] Sylvain Hamman,[a] Eric Saint-Aman,[b] and Jean-Louis Pierre[a]

Abstract: Four tripodal ligands with an N_3O coordination sphere were synthesized: (2-hydroxy-3-*tert*-butyl-5-nitrobenzyl)bis(2-pyridylmethyl)amine (LNO_2H), (2-hydroxy-3-*tert*-butyl-5-fluorobenzyl)bis(2-pyridylmethyl)amine (LFH), (2-hydroxy-3,5-di-*tert*-butylbenzyl)bis(2-pyridylmethyl)amine (L*t*BuH) and (2-hydroxy-3-*tert*-butyl-5-methoxybenzyl)bis(2-pyridylmethyl)amine (LOMeH). Their square-pyramidal copper(II) complexes, in which the phenol subunit occupies an axial position, were prepared and characterized by X-ray crystallography and UV/Vis and EPR spectroscopy. The phenolate moieties of the copper(II) complexes of L*t*BuH and LOMeH were electrochemically oxidized to phenoxyl radicals. These complexes are EPR-active ($S=1$), highly stable ($k_{decay}=0.008\,min^{-1}$ for $[Cu^{II}(LOMe^{\bullet})(CH_3CN)]^{2+}$) and stoichiometrically oxidise benzyl alcohol. Two additional tripodal ligands providing an N_2O_2 coordination sphere were also studied: (2-pyridylmethyl)(2-hydroxy-3-*tert*-butyl-5-methoxybenzyl)-(2-hydroxy-3-*tert*-butyl-5-nitrobenzyl)-amine ($L'OMeNO_2H_2$) and (2-pyridylmethyl)bis(2-hydroxy-3-*tert*-butyl-5-methoxy)benzylamine ($L'OMe_2H_2$). Their copper(II) complexes were isolated as dimers ($[Cu^{II}_2(L'OMe_2)_2]$, $[Cu^{II}_2(L'OMeNO_2)_2]$) that are converted to monomers on addition of pyridine. The complexes were investigated by X-ray crystallography and UV/Vis and EPR spectroscopy. Their one-electron electrochemical oxidation leads to copper(II) – phenoxyl systems that are less stable than those of the N_3O complexes. The N_2O_2 complexes are more reactive than the N_3O analogues: they aerobically oxidize benzyl alcohol to benzaldehyde at a higher rate, as well as ethanol to acetaldehyde (40 – 80 turnovers).

Keywords: enzyme models · copper · oxidation · tripodal ligands · radicals

Introduction

Various strategies are used by metalloenzymes to store oxidizing equivalents required for multi-electron transfers. A fascinating class of metalloenzymes use an organic redox center (free radical) on their own polypeptide chain to provide or abstract electrons and complete metal-driven electron transfer in the catalytic process.[1] Galactose oxidase (GOase), an enzyme typical of this class, is an extracellular type II copper protein (68 kDa) of fungal origin that catalyzes the oxidation of a broad range of primary alcohols to aldehydes with concomitant reduction of molecular oxygen.[2] The crystal structure of GOase contains a square-pyramidal copper ion with a tyrosinate or protonated tyrosinate ligand weakly bound in the axial position, two histidine imidazole units, a second tyrosinate and either H_2O or acetate (replacing the substrate) in the equatorial sites (Scheme 1).[3] The equatorial tyrosinate group is linked to a nearby cysteine residue by an ortho C–S bond. The enzyme exists in three well-defined and stable oxidation states [Eq. (1)]: the EPR-silent active oxidized form, in which a copper(II) ion is antiferromagnetically coupled to an equatorial tyrosyl radical responsible for hydrogen atom abstraction from the substrate; the intermediate copper(II) form; and the reduced form, which contains a copper(I) center.

$$Cu^{II}\text{–}O^{\bullet+}Tyr \rightleftharpoons Cu^{II}\text{–}OTyr \rightleftharpoons Cu^{I}\text{–}OTyr \quad (1)$$

The axial tyrosine residue is involved in a protonation–deprotonation process during the catalytic cycle (Scheme 1). Recent theoretical studies[4] showed that, prior to proton transfer from substrate to enzyme, the radical is located at the axial tyrosinate site. The radical is shifted to the equatorial tyrosinate group simultaneously with proton transfer.

Several models of the active site of GOase have been prepared in the last few years to give an insight into the structure and properties of its reactive center.[5] Tripodal

[a] Dr. F. Thomas, A. Philibert, Dr. C. Philouze, Dr. S. Hamman, Prof. Dr. J.-L. Pierre
Laboratoire de Chimie Biomimétique, LEDSS, UMR CNRS 5616
Université J. Fourier, BP 53, 38041, Grenoble Cedex 9 (France)
Fax: (+33) 4-76-51-48-36
E-mail: Fabrice.Thomas@ujf-grenoble.fr

[b] Prof. Dr. E. Saint-Aman
LEOPR, UMR CNRS 5630, Université J. Fourier
BP 53, 38041 Grenoble Cedex 9 (France)

Supporting information for this article is available on the WWW under http://www.chemeurj.org/ or from the author.

 DOI: 10.1002/chem.200304880

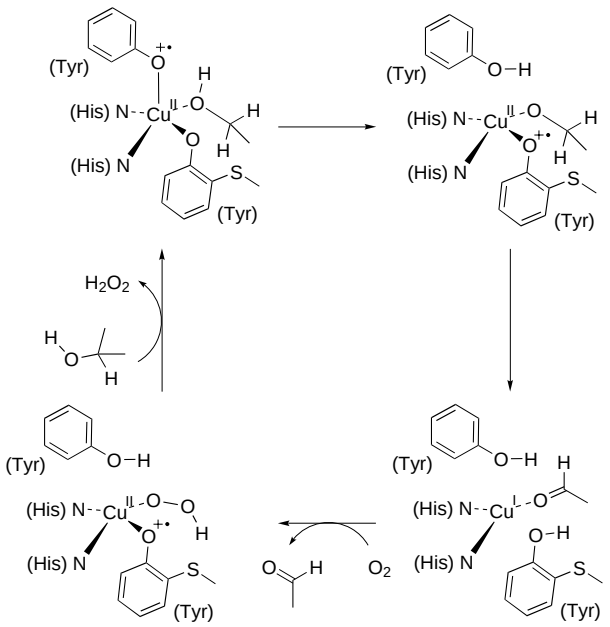

Scheme 1. The galactose oxidase active site and adaptation of the catalytic pathway proposed by F. Himo et al.[4a]

ligands have been commonly used to provide a coordination sphere similar to that of the enzyme. Some involve an N_3O coordination sphere[6] (usually two pyridine nitrogen atoms, one tertiary amine nitrogen atom and one phenolic oxygen atom), and others an N_2O_2 coordination sphere[7] (usually one pyridine nitrogen atom, one tertiary amine nitrogen atom and two phenolic oxygen atoms). However, very few of these models exhibit catalytic activity. One of the trickiest problems encountered in the design of biomimetic models for the Cu^{II}–phenoxyl radical active form is the control of the radical center. This control, which involves stability, magnetic properties and reactivity, depends on interdependent factors such as protonation of the phenolic moieties, geometry (axial versus equatorial binding to copper) and electronic properties.

Here we compare the solution chemistry, the stability of the phenoxyl radicals and the catalytic properties of copper(II) complexes prepared from N_2O_2 and N_3O ligands (Scheme 2). The four N_3O ligands have a phenolic arm that is substituted in the *para* position by electron-donating or electron-withdrawing groups. In a complex of a related non-*tert*-butylated ligand the nitrophenolate group occupies an axial position,[8] and this suggests that the phenolate group of the corresponding *tert*-butylated ligand will also occupy an axial position in its copper complex. In a preliminary report, we described a

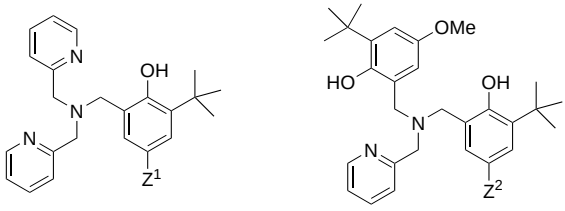

Z^1= OMe (LOMeH), *t*Bu (L*t*BuH), F (LFH), NO_2 (LNO_2H)

Z^2= OMe ($L'OMe_2H_2$), NO_2 ($L'OMeNO_2H_2$)

Scheme 2. Chemical structures of the ligands.

functional model involving two different phenolic arms in a tripodal N_2O_2 ligand and obtained a radical center located on the equatorial phenolic arm.[9]

Results and Discussion

Preparation of the ligands: L*t*BuH has been previously described.[6f] We improved the synthesis by using a Mannich reaction: in a one-pot synthesis L*t*BuH was obtained by mixing bis(2-pyridylmethyl)amine and 2,4-di-*tert*-butyl-4-phenol in the presence of one equivalent of formaldehyde. The Mannich reaction was also used to prepare LOMeH and LFH. Alkylation of bis(2-pyridylmethyl)amine with 2-bromomethyl-6-*tert*-butyl-4-nitrophenyl acetate was the preferred method for obtaining LNO_2H. Synthesis of the N_2O_2 ligands $L'OMeNO_2H_2$ and $L'OMe_2H_2$ has been previously described.[10]

Copper complexes: *N_2O_2 ligands*: On mixing $Cu(ClO_4)_2 \cdot 6H_2O$ and the N_2O_2 ligands in acetonitrile in the presence of NEt_3, a dimeric species was obtained (Scheme 3). Single crystals of $[Cu^{II}_2(L'OMe_2)_2]$ suitable for X-ray diffraction

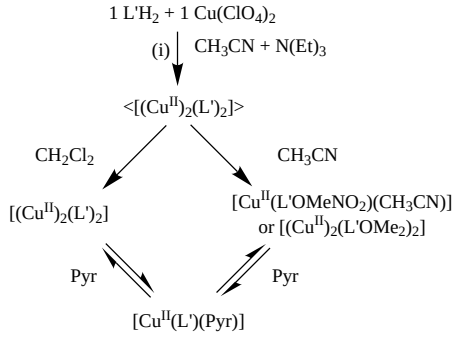

Scheme 3. Solution chemistry of the N_2O_2 ligands, where L′ represents $L'OMe_2$ or $L'OMeNO_2$ (i: [L] > 0.05 M).

studies were obtained by recrystallization from acetonitrile after 12 h at 277 K (Table 1). The crystal structure of $[Cu^{II}_2(L'OMe_2)_2]$ is depicted in Figure 1, and selected bond angles and lengths are reported in Table 2. The two copper atoms have similar pentacoordinate environments that share two oxygen atoms from two ligands. The geometry around the copper(II) center is intermediate between trigonal-bipyramidal and square-pyramidal, as reflected by a τ value[11] of 0.35. Each copper atom is coordinated to two nitrogen and three oxygen atoms: the pyridine nitrogen atom (N2), the tertiary amino nitrogen atom (N1), one phenolate oxygen atom (O2) and two μ-phenoxo oxygen atoms (O1, O1′). The Cu–O2 bond length (1.895(3) Å) is shorter than Cu–O1′ (1.984(3) Å or Cu–O1 2.045(2) Å); the O1-Cu-O1′ angle (73.8°) is significantly different from the Cu-O1-Cu angle (90.8°). Consequently, the CuOCuO unit is not flattened, but shows a butterfly structure with a dihedral angle of 126.5° and a short copper–copper distance of 2.869 Å.

In $[Cu^{II}_2(L'OMeNO_2)_2]$, which was previously reported but not described,[9] the same geometry was observed ($\tau = 0.34$

Table 1. Crystallographic data for $[Cu^{II}(LtBuH)(CH_3CN)](ClO_4)_2$, $[Cu^{II}(LOMeH)(CH_3CN)](ClO_4)_2$, $[Cu^{II}(LFH)(CH_3CN)](ClO_4)_2$, $[Cu^{II}(LNO_2H)(CH_3CN)](ClO_4)_2$, $[Cu^{II}(LNO_2)(Cl)]$ and $[Cu^{II}_2(L'OMe_2)_2]$.

	$[Cu^{II}_2(L'OMe_2)_2]$	$[Cu^{II}(LtBuH)(CH_3CN)]\ (ClO_4)_2$	$[Cu^{II}(LNO_2)(Cl)]$
formula	$C_{60}H_{76}Cu_2N_4O_8$	$C_{29}H_{38}Cl_2CuN_4O_9$	$C_{23}H_{25}ClCuN_4O_3$
M	1108.37	721.09	504.47
symmetry	monoclinic	monoclinic	triclinic
morphology	brown prism	blue platelet	dark green platelet
crystal dimensions [mm]	$0.41 \times 0.37 \times 0.25$	$0.48 \times 0.45 \times 0.25$	$0.39 \times 0.35 \times 0.17$
a [Å]	28.49(3)	13.2504(6)	8.2328(6)
b [Å]	9.690(4)	11.745(1)	11.9330(9)
c [Å]	27.72(3)	22.804(3)	12.3562(6)
α [°]	90	90	70.5(3)
β [°]	131.1(1)	97.7(4)	80.7(3)
γ [°]	90	90	73.9(3)
V [Å^3]	5770(10)	3517(2)	1097(2)
T [K]	293.0	293.0	150.0
space group	$C2/c$	$P2_1/a$	$P\bar{1}$
Z	4	4	2
monochromator	graphite	graphite	graphite
$\lambda(Mo_{K\alpha})$ [Å]	0.71073	0.71073	0.71073
γ [mm^{-1}]	0.793	0.826	1.152
no. of reflections (measured)	12727	46219	12569
no. of reflections (unique)	6433	8150	4481
no. of reflections	3090 ($I > 2\sigma$)	3398 ($I > 1.5\sigma$)	3262 ($I > 3\sigma$)
R_{int}	0.148	0.211	0.039
R	0.073	0.063	0.036
$R(w)$	0.060	0.068	0.042
	$[Cu^{II}(LFH)(CH_3CN)](ClO_4)_2$	$[Cu^{II}(LOMeH)(CH_3CN)](ClO_4)_2$	$[Cu^{II}(LNO_2H)(CH_3CN)](ClO_4)_2$
formula	$C_{25}H_{29}Cl_2CuFN_4O_9$	$C_{26}H_{32}Cl_2CuN_4O_{10}$	$C_{28}H_{33}Cl_2CuN_5O_{11}$
M	682.98	726.30	764.56
symmetry	triclinic	triclinic	triclinic
morphology	blue prism	blue block	blue-green prism
crystal dimensions [mm]	$0.48 \times 0.28 \times 0.15$	$0.28 \times 0.18 \times 0.16$	$0.76 \times 0.61 \times 0.58$
a [Å]	8.2493(3)	8.2869(2)	9.9996(5)
b [Å]	9.5464(4)	9.4031(4)	11.0806(9)
c [Å]	19.0287(9)	20.3281(8)	15.6455(9)
α [°]	93.8(2)	80.9(2)	99.4(4)
β [°]	99.1(2)	78.8(1)	98.0(2)
γ [°]	100.9(2)	80.3(1)	98.7(3)
V [Å^3]	1446(1)	1518.8(9)	1666(3)
T [K]	293.0	293.0	150.0
space group	$P\bar{1}$	$P\bar{1}$	$P\bar{1}$
Z	2	2	2
monochromator	graphite	graphite	graphite
$\lambda(Mo_{K\alpha})$ [Å]	0.71073	0.71073	0.71073
μ [mm^{-1}]	1.005	0.955	0.883
no. of reflections (measured)	21596	18879	13014
no. of reflections (unique)	8029	8693	7110
no. of reflections	4387 ($I > 3\sigma$)	5170 ($I > 2\sigma$)	5904 ($I > 2\sigma$)
R_{int}	0.081	0.074	0.040
R	0.059	0.057	0.052
$R(w)$	0.093	0.076	0.086

and 0.39 for the two copper(II) centers) with a bridging methoxyphenolate and a nonbridging nitrophenolate group: the electron-donating methoxyl group compensates more efficiently than the nitro group for the electron deficiency on the bridging oxygen atom. The substitution thus orientates the position of the phenolate groups in these dimers according to their electronic properties.

$[Cu^{II}_2(L'OMeNO_2)_2]$ and $[Cu^{II}_2(L'OMe_2)_2]$ are EPR-silent in the noncoordinating solvent CH_2Cl_2 due to strong coupling between the two Cu^{II} centers mediated by the phenolato bridge.[7d] Dissolving $[Cu^{II}_2(L'OMeNO_2)_2]$ in acetonitrile results in the appearance of an EPR signal typical for a mononuclear copper complex. However, no EPR signal was observed after dissolution of $[Cu^{II}_2(L'OMe_2)_2]$ in acetonitrile. The dimeric complex $[Cu^{II}_2(L'OMe_2)_2]$ can be converted to the monomeric species by addition of a coordinating base such as pyridine (Pyr). Titration of the dimers with pyridine was monitored by UV/Vis spectroscopy: the intensity of the ligand to metal charge-transfer (LMCT) band in the dimers was higher than in the monomers, while a shift in λ_{max} was observed (Table 3). From the equilibrium of Equation (2)

$$L'_2Cu_2 + 2\,Pyr \overset{K^{Pyr}}{\rightleftharpoons} 2\,L'CuPyr \qquad (2)$$

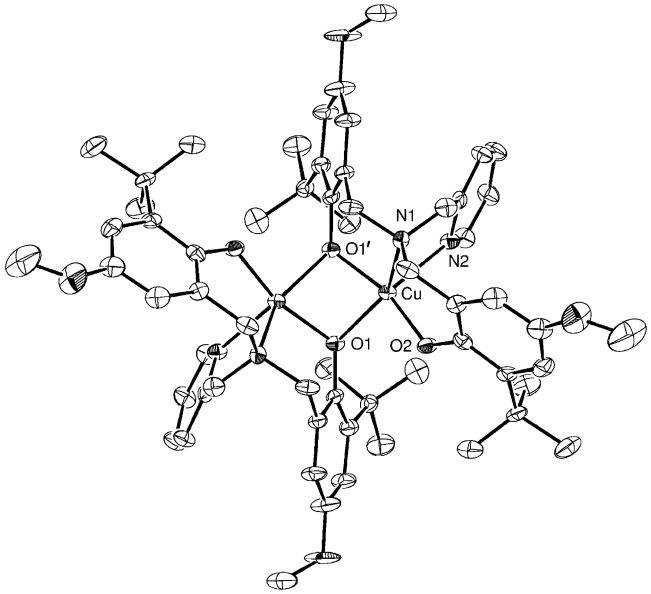

Figure 1. ORTEP plot showing 25% displacement ellipsoids and partial atomic labeling for $[Cu^{II}_2(L'OMe_2)_2]$. Hydrogen atoms have been omitted for clarity; selected distances and angles are reported in Table 2.

where L′ = ligand and $K^{pyr} = [Cu^{II}(L')(Pyr)]^2/([Cu^{II}_2(L')_2][Pyr]^2)$, we obtained $K^{pyr}[Cu^{II}_2(L'OMeNO_2)_2] = 10^{3.7}\,M^{-1}$ and $K^{pyr}[Cu^{II}_2(L'OMe_2)_2] = 10^{2.3}\,M^{-1}$.

This confirmed the easier cleavage of the dimeric structure $[Cu^{II}_2(L'OMeNO_2)_2]$. These results cannot be explained on the basis of the X-ray analysis, which shows a butterfly structure for both dimers and similar interatomic distances. However, nitro as opposed to methoxyl substitution makes the coordinated Cu^{II} atom more electrophilic and thus favors nucleophilic attack by pyridine. The solution chemistry of the N_2O_2 ligands in the presence of copper(II) is summarized in Scheme 3.

N_3O ligands: The solution chemistry of the copper(II) complexes of the N_3O ligands differs notably from that of their N_2O_2 analogues (Scheme 4). Monomeric complexes were obtained on mixing stoichiometric amounts of the N_3O ligands and $Cu(ClO_4)_2\cdot 6H_2O$ in acetonitrile in the presence of NEt_3. Under these conditions the complexes were isolated in their protonated form, in which the phenolic subunit remains protonated and only d–d transitions are observed in the visible spectrum. The ligand LNO_2H was an exception: $[Cu^{II}(LNO_2H)(CH_3CN)]^{2+}$ was obtained in the absence of base.

Blue single crystals of $[Cu^{II}(LOMeH)(CH_3CN)]^{2+}$, $[Cu^{II}(LtBuH)(CH_3CN)]^{2+}$ and $[Cu^{II}(LFH)(CH_3CN)]^{2+}$ were obtained on slow diffusion of di-*n*-butyl ether into solutions of the complexes in acetonitrile. For $[Cu^{II}(LNO_2H)(CH_3CN)]^{2+}$ toluene was used instead of di-*n*-butyl ether. The ORTEP plots of their structures are depicted in Figure 2; selected bond lengths and angles are listed in Table 2.

The geometry around the metal centers is square-pyramidal with a phenolic unit that weakly coordinates the copper atom in an axial position.

In $[Cu^{II}(LOMeH)(CH_3CN)]^{2+}$ the copper atom is coordinated in the square plane by one tertiary nitrogen atom N1,

Table 2. Selected bond lengths [Å] and angles [°] of the complexes $[Cu^{II}(LtBuH)(CH_3CN)](ClO_4)_2$, $[Cu^{II}(LOMeH)(CH_3CN)](ClO_4)_2$, $[Cu^{II}(LFH)(CH_3CN)](ClO_4)_2$, $[Cu^{II}(LNO_2H)(CH_3CN)](ClO_4)_2$, $[Cu^{II}(LNO_2)(Cl)]$ and $[Cu^{II}_2(L'OMe_2)_2]$.

	$[Cu^{II}(LtBuH)(CH_3CN)]$	
Cu–O1 2.456(3)	Cu–N1 2.037(4)	Cu–N2 1.987(4)
Cu–N3 1.977(4)	Cu–N4 1.974(6)	
O1-Cu-N1 90.5(1)	O1-Cu-N2 97.2(1)	O1-Cu-N3 91.6(1)
O1-Cu-N4 90.5(2)	N1-Cu-N2 83.4(2)	N1-Cu-N3 83.6(2)
N1-Cu-N4 178.5(2)	N2-Cu-N3 164.4(2)	N2-Cu-N4 95.4(2)
N3-Cu-N4 97.4(2)		
	$[Cu^{II}(LFH)(CH_3CN)]$	
Cu–O1 2.404(3)	Cu–N1 2.024(4)	Cu–N2 1.976(4)
Cu–N3 1.975(3)	Cu–N4 2.008(4)	
O1-Cu-N1 89.8(1)	O1-Cu-N2 98.0(1)	O1-Cu-N3 92.6(1)
O1-Cu-N4 92.6(1)	N1-Cu-N2 83.7(2)	N1-Cu-N3 84.0(1)
N1-Cu-N4 177.4(2)	N2-Cu-N3 163.6(1)	N2-Cu-N4 95.0(2)
N3-Cu-N4 96.9(2)		
	$[Cu^{II}(LOMeH)(CH_3CN)]$	
Cu–O1 2.411(2)	Cu–N1 2.028(3)	Cu–N2 1.983(3)
Cu–N3 1.974(3)	Cu–N4 2.002(3)	
O1-Cu-N1 89.9(1)	O1-Cu-N2 98.2(1)	O1-Cu-N3 91.1(1)
O1-Cu-N4 93.3(1)	N1-Cu-N2 83.3(1)	N1-Cu-N3 84.3(1)
N1-Cu-N4 176.4(1)	N2-Cu-N3 164.4(1)	N2-Cu-N4 94.6(1)
N3-Cu-N4 97.3(1)		
	$[Cu^{II}(LNO_2H)(CH_3CN)]$	
Cu–O1 2.430(2)	Cu–N1 2.014(2)	Cu–N2 1.989(2)
Cu–N3 1.988(2)	Cu–N4 1.962(2)	
O1-Cu-N1 87.14(7)	O1-Cu-N2 88.23(8)	O1-Cu-N3 92.87(8)
O1-Cu-N4 95.03(8)	N1-Cu-N2 83.84(8)	N1-Cu-N3 82.18(9)
N1-Cu-N4 177.46(9)	N2-Cu-N3 165.91(9)	N2-Cu-N4 97.52(9)
N3-Cu-N4 96.4(1)		
	$[Cu^{II}(LNO_2)(Cl)]$	
Cu–Cl 2.2651(7)	Cu–O1 2.190(2)	Cu–N1 2.057(2)
Cu–N2 1.994(2)	Cu–N3 1.996(2)	
Cl-Cu-O1 97.38(5)	Cl-Cu-N1 170.33(6)	Cl-Cu-N2 95.53(6)
Cl-Cu-N3 95.81(6)	O1-Cu-N1 92.29(7)	O1-Cu-N2 102.44(8)
O1-Cu-N3 95.66(8)	N1-Cu-N2 82.35(8)	N1-Cu-N3 83.16(8)
N2-Cu-N3 157.18(9)		
	$[Cu^{II}_2(L'OMe_2)_2]$	
Cu–O1′ 1.984(3)	Cu–O1 2.045(2)	Cu–O2 1.895(3)
Cu–N1 2.126(3)	Cu–N2 2.284(3)	Cu–Cu 2.869(3)
O1-Cu-O1′ 73.8(1)	O1′-Cu-O2 165.1(1)	O1′-Cu-N1 93.7(1)
O1′-Cu-N2 92.0(1)	O1-Cu-O2 93.1(1)	O1-Cu-N1 144.5(1)
O1-Cu-N2 132.4(1)	O2-Cu-N1 93.2(1)	O2-Cu-N2 102.2(1)
N1-Cu-N2 79.8(1)	Cu-O1-Cu 90.8(1)	

Table 3. Electronic properties of the copper(II) complexes in acetonitrile solution (UV/Vis spectra recorded at 298 K).

Complex	λ_{max} [nm] (ε [$M^{-1}cm^{-1}$])
$[Cu^{II}(LOMeH)(CH_3CN)]^{2+}$	400 (320),[a] 590 (230)[a]
$[Cu^{II}(LOMe)(CH_3CN)]^{+}$	565 (1040)
$[Cu^{II}(LOMe)(Pyr)]^{+}$	546 (950)
$[Cu^{II}(LtBuH)(CH_3CN)]^{2+}$	600 (180)[a]
$[Cu^{II}(LtBu)(CH_3CN)]^{+}$	553 (935), 950 (180)[a]
$[Cu^{II}(LtBu)(Pyr)]^{+}$	531 (750), 850 (180)[a]
$[Cu^{II}(LFH)(CH_3CN)]^{2+}$	550 (240)
$[Cu^{II}(LF)(CH_3CN)]^{+}$	305 (3400), 535 (920), 930 (130)[a]
$[Cu^{II}(LF)(Pyr)]^{+}$	309 (3800), 514 (780), 870 (140)[a]
$[Cu^{II}(LNO_2H)(CH_3CN)]^{2+}$	388 (14830), 606 (90)
$[Cu^{II}(LNO_2)(CH_3CN)]^{+}$	390 (11200), 517 (636)
$[Cu^{II}(LNO_2)(Pyr)]^{+}$	396 (17280), 500 (401),[b] 644 (139), 868 (130)
$[Cu^{II}(L'OMeNO_2H)(OAc)]$	298 (10300), 393 (20000), 500 (760),[b] 600 (510)[a]
$[Cu^{II}_2(L'OMeNO_2)_2]$	296 (11400), 391 (28100), 500 (5100)[b]
$[Cu^{II}(L'OMeNO_2)(Pyr)]$	305 (6300), 401 (15000), 500 (1210),[b] 700 (300)[a]
$[Cu^{II}_2(L'OMe)_2]$	302 (16700), 445 (4330), 650 (1600)[a]
$[Cu^{II}(L'OMe_2)(Pyr)]$	310 (20000), 488 (1400)

[a] Broad absorption. [b] Shoulder.

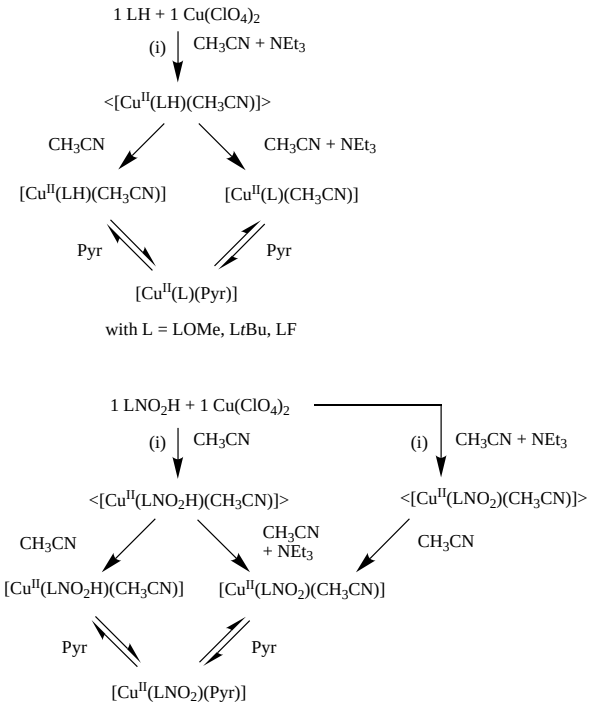

Scheme 4. Solution chemistry of the N_3O ligands (i: [L] > 0.05 M).

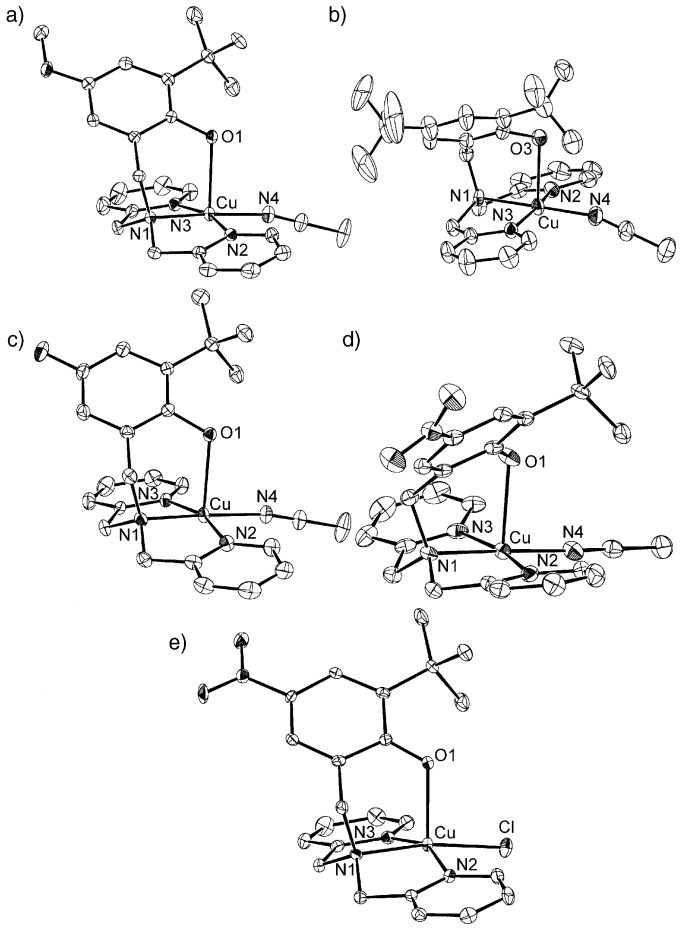

Figure 2. ORTEP plots showing 25% (a, b, c) or 50% (d, e) displacement ellipsoids and partial atomic labeling for $[Cu^{II}(LOMeH)(CH_3CN)]^{2+}$ (a), $Cu^{II}(LtBuH)(CH_3CN)]^{2+}$ (b), $[Cu^{II}(LFH)(CH_3CN)]^{2+}$ (c), $[Cu^{II}(LNO_2H)(CH_3CN)]^{2+}$ (d) and $[Cu^{II}(LNO_2)(Cl)]$ (e). Hydrogen atoms have been omitted for clarity; selected distances and angles are reported in Table 3.

two pyridine nitrogen atoms N2 and N3 and one acetonitrile nitrogen atom N4, with copper–nitrogen bond lengths of 2.028(3) (N1), 1.983(3) (N2), 1.974(3) (N3) and 2.002(3) Å (N4). The Cu–O1 distance of 2.411(2) Å is significantly longer than those reported for axially coordinated phenolates.[8] It is within the range of that (2.567 Å) reported for the protonated complex $[Cu^{II}(LtBuH)(Cl)]^+$ bearing a chloride ion as an exogenous ligand in place of acetonitrile.[6f] The protonated phenolic unit thus binds weakly to the copper atom, which lies 0.120(3) Å above the basal plane and towards the axial O1 atom. The coordination modes of $[Cu^{II}(LtBuH)(CH_3CN)]^{2+}$, $[Cu^{II}(LFH)(CH_3CN)]^{2+}$ and $[Cu^{II}(LNO_2H)(CH_3CN)]^{2+}$ are similar to that of $[Cu^{II}(LOMeH)(CH_3CN)]^{2+}$, with Cu–O1 distances of 2.456(3), 2.404(3) and 2.430(2) Å, respectively. The Cu–N2 and Cu–N3 distances range between 1.975(3) and 1.989(2) Å, the Cu–N1 distances between 2.014(2) and 2.037(4) Å and the Cu–N4 distances between 1.962(2) and 2.008(4) Å.

The copper(II) complex of LNO_2H could also be prepared in its deprotonated form $[Cu^{II}(LNO_2)(CH_3CN)]^+$ by mixing stoichiometric amounts of $Cu(ClO_4)_2 \cdot 6H_2O$ and $HLNO_2$ in acetonitrile in the presence of one equivalent of NEt_3. Slow diffusion of diethyl ether into this solution afforded dark green crystals of $[Cu^{II}(LNO_2)(CH_3CN)]^+$, which, however, were not suitable for X-ray analysis. To obtain single crystals suitable for a X-ray analysis, CuCl must be used instead of $Cu(ClO_4)_2 \cdot 6H_2O$ to prepare the complex.[12] Based on the structural similarity between $[Cu^{II}(LtBuH)(CH_3CN)]^{2+}$ and $[Cu^{II}(LtBuH)(Cl)]^+$,[6f] no significant geometrical changes are expected when acetonitrile is replaced by a chloro ligand. The geometry around the copper atom in $[Cu^{II}(LNO_2)(Cl)]$ can be described as square-pyramidal. The Cu–O1 distance in $[Cu^{II}(LNO_2)(Cl)]$ differs from those of $[Cu^{II}(LNO_2H)(CH_3CN)]^{2+}$ and $[Cu^{II}(LOMeH)(CH_3CN)]^{2+}$. It is significantly shorter (2.190(2) Å) and within the range of those reported for axially coordinated phenolates.[8] The copper atom is displaced 0.235(2) Å above the basal plane towards the axial oxygen atom, as expected for a stronger Cu–O1 bond (0.036(2) Å in $[Cu^{II}(LNO_2H)(CH_3CN)]^{2+}$). The bond lengths between the copper atom and the donor nitrogen atoms are Cu–N1 2.057(2), Cu–N2 1.994(2) and Cu–N3 1.996(2) Å, and the Cu–Cl bond length is 2.2651(7) Å. An axial position of the nitrophenolate moiety was already observed in a related complex[8] and explained[5a] in terms of the short methylene spacer between the pyridine and tertiary amino groups: the two five-membered chelate rings are preferentially located in the basal plane. The deprotonated complexes of the other N_3O ligands bearing electron-donating substituents could not be isolated in the solid state, even in the presence of NEt_3, due to their higher pK_a.

After dissolution of the protonated complexes in acetonitrile (Scheme 4), only d–d transitions were observed in the visible region of the electronic spectrum (Table 3); this suggests that the phenolic subunit remains protonated in solution. The EPR spectrum reveals a mononuclear Cu^{II} complex. On addition of one equivalent of NEt_3 the solution turns violet; the UV/Vis spectrum shows emergence of an LMCT transition (the electron-withdrawing NO_2 group induces a hypsochromic shift, while the electron-donating

groups *t*Bu and OMe induce a bathochromic shift); this indicates that the weakly coordinating phenolic arm is deprotonated on addition of NEt_3 and coordinates to the copper atom. Use of excess pyridine (50 equiv) in place of NEt_3 also results in the appearance of phenolate to copper charge-transfer band at a somewhat shorter wavelength, which indicates that pyridine acts both as a base and as an exogenous ligand. The solution chemistry of the copper complexes of N_3O ligands is summarized in Scheme 4.

Electrochemistry of the protonated ligands and complexes: The electrochemical behaviour of the protonated ligands and complexes was studied in acetonitrile by cyclic voltammetry (CV). Only the results obtained with N_3O ligands are presented. The electrochemistry of the N_2O_2 ligands was previously described.[10]

The CV curve of the free ligands displays irreversible anodic signals, as expected for phenol-centered electron transfer. Oxidation of the nitrophenol to its phenoxyl radical occurs at the highest potential (+0.65 V versus Fc/Fc^+); the fluorine-substituted phenol has an oxidation potential (+0.46 V) close to that of an unfluorinated parent compound,[10] and the *t*Bu- and OMe-substituted phenols have the lowest oxidation potentials (+0.37 and +0.29 V, respectively), in agreement with the electron-donating properties of their substituents: A plot of E_p^a as a function of the Hammet constants σ^+ shows a linear dependence (Supporting Information).

The CV curves of all the protonated complexes show irreversible redox signals around +0.8 V. These values are close to that previously reported by Shimazaki et al.[6f] for $[Cu^{II}(LtBuH)(Cl)]^{2+}$. Oxidation occurs at higher potentials relative to the free ligands due to the positive charge on the copper atom, which decreases the electron density on the phenolic unit and thus makes it less easily oxidizable.

Radical generation in the deprotonated complexes: The electrochemical behaviour of $[Cu^{II}(LNO_2)(CH_3CN)]^+$ and $[Cu^{II}(LNO_2)(Pyr)]^+$ is characterized by a signal at $E_{1/2} = +0.70$ V. It is not fully reversible ($i_{Pa}/i_{Pc} > 1$) even at low temperature (233 K), which suggests a relatively low stability of the oxidized species. Coulometric titration revealed a one-electron process. Dramatic changes in the electronic spectrum were observed during electrolysis: the 390 nm absorption ($\varepsilon = 11200\,M^{-1}cm^{-1}$), attributed to the $\pi-\pi^*$ transition of the nitrophenolate, is strongly modified ($\lambda_{max} = 387$ nm, $\varepsilon = 6400\,M^{-1}cm^{-1}$; shoulder at 440 nm, $\varepsilon = 3900\,M^{-1}cm^{-1}$), while the LMCT transition at 517 nm disappears. These results strongly suggest the formation of a transient nitrophenoxyl species. Assuming that no isomerization occurs during electrolysis, this is a good example of a phenoxyl radical axially coordinated to a metal atom. Its low stability, however, precluded further characterization.

The CV curves of $[Cu^{II}(LF)(CH_3CN)]^+$ and $[Cu^{II}(LF)(Pyr)]^+$ at room temperature reveal a redox couple that is not fully reversible ($i_{Pa}/i_{Pc} > 1$) at +0.20 V. When the temperature is lowered to 233 K, a total loss of reversibility is observed, and only the anodic peak is seen on the CV curve; this is likely due to the formation of passivating ion pairs between the oxidized complex (charge: +2) and the perchlorate anions of the supporting electrolyte (TBAP). Under these conditions, electrolysis could not be performed.[13]

The CV curves of $[Cu^{II}(LOMe)(Pyr)]^+$, $[Cu^{II}(LOMe)(CH_3CN)]^+$, $[Cu^{II}(LtBu)(Pyr)]^+$, $[Cu^{II}(LtBu)(CH_3CN)]^+$, $[Cu^{II}(L'OMe_2)(Pyr)]$ and $[Cu^{II}(L'OMeNO_2)(Pyr)]$ reveal reversible one-electron (as estimated by coulometric titration) redox waves at +0.02, +0.01, +0.17, +0.15, −0.16, and −0.08 V, respectively. No significant change in $E_{1/2}$ was observed for the N_3O complexes when the exogenous pyridine ligand was replaced by acetonitrile, as also observed by Taki et al.[7a] As expected, oxidation occurs on the methoxyphenolate moieties of $[Cu^{II}(L'OMeNO_2)(Pyr)]$, with a $E_{1/2}$ value close to that obtained for $[Cu^{II}(L'OMe_2)(Pyr)]$.

The EPR spectra of the electrogenerated species $[Cu^{II}(LOMe^{\bullet})(Pyr)]^{2+}$, $[Cu^{II}(LOMe^{\bullet})(CH_3CN)]^{2+}$, $[Cu^{II}(LtBu^{\bullet})(Pyr)]^{2+}$, $[Cu^{II}(LtBu^{\bullet})(CH_3CN)]^{2+}$, $[Cu^{II}(L'OMe_2^{\bullet})(Pyr)]^+$ and $[Cu^{II}(L'OMeNO_2^{\bullet})(Pyr)]^+$ show a $\Delta M_S = \pm 2$ signal centred at 150 mT, associated with $\Delta M_S = \pm 1$ transitions typical of an $S = 1$ system (Figure 3). The UV/Vis spectra

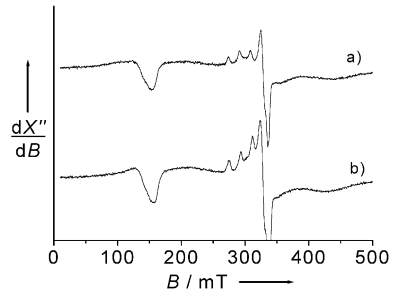

Figure 3. X-band EPR spectra of the electrochemically generated complexes $[Cu^{II}(LOMe^{\bullet})(Pyr)]^{2+}$ (a) and $[Cu^{II}(L'OMeNO_2^{\bullet})(Pyr)]^+$ (b); a contaminant with $S = 1/2$ (accounting for less than 5 (a) or 10% (b) of the total copper(II) concentration) corresponding to a monomeric Cu^{II} complex is also present; $[Cu^{II}(LOMe^{\bullet})(Pyr)]^{2+} = [Cu^{II}(L'OMeNO_2^{\bullet})(Pyr)]^+ = 2$ mM, $T = 4$ K, 9.44711 GHz, 0.25 mW; modulation 0.5 mT, 100 KHz.

of these oxidized species show sharp and intense absorptions at around 420 nm (Figure 4, Table 4), as previously observed for phenoxyl radicals,[14] and attributed to $\pi-\pi^*$ transitions. The LMCT transitions are no longer present in the 500–600 nm region. Taken together, these results unambiguously show evidence for the formation of a phenoxyl radical that is ferromagnetically coupled to the copper(II) center.

Both $[Cu^{II}(LOMe^{\bullet})(CH_3CN)]^{2+}$ and $[Cu^{II}(LOMe^{\bullet})(Pyr)]^{2+}$ were found to be highly stable at 298 K ($k_{decay} = 0.008$ and $0.0045\,min^{-1}$ respectively). To our knowledge, only one Cu^{II}–phenoxyl radical possessing such a stability has been recently described in literature.[6d] The other radical complexes are relatively stable at 298 K: $k_{decay} = 0.155$ ($[Cu^{II}(LOMeNO_2^{\bullet})(Pyr)]^+$), 0.155 ($[Cu^{II}(LtBu^{\bullet})(CH_3CN)]^{2+}$) and $0.087\,min^{-1}$ ($[Cu^{II}(LtBu^{\bullet})(Pyr)]^{2+}$). The exogenous pyridine ligand greatly stabilizes the radical. In the case of the N_3O complexes, the lower the redox potential, the longer the half-life of the radical (Table 4), while an inverse correlation is observed with N_2O_2 complexes. Moreover, the radical complexes of the N_3O ligands are more stable than those of the N_2O_2 ligands. In $[Cu^{II}(L'OMeNO_2^{\bullet})(Pyr)]^+$, the presence of a

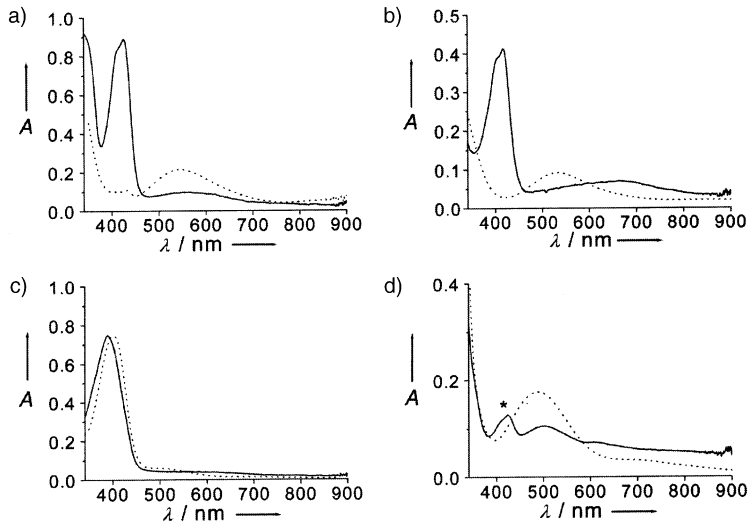

Figure 4. UV/Vis spectra of the copper complexes (dotted lines) and the corresponding electrogenerated Cu^{II}–phenoxyl radical complexes (solid lines): $[Cu^{II}(LOMe^{\bullet})(Pyr)]^{2+}$ 0.11×10^{-3} M (a), $[Cu^{II}(L{\it t}Bu^{\bullet})(Pyr)]^{2+}$ 0.11×10^{-3} M (b), $[Cu^{II}(L'OMeNO_2^{\bullet})(Pyr)]^{+}$ 0.05×10^{-3} M (c), $[Cu^{II}(L'OMe_2^{\bullet})(Pyr)]^{2+}$ 0.11×10^{-3} M (d); spectra recorded in acetonitrile (+0.01 M TBAP) at 233 K in a 1 cm path length quartz cell; * denotes an underestimated transient absorption due to instability of the complex, even at 233 K.

nitrophenolate goup coordinated to the copper atom stabilizes the radical generated on the methoxyphenolate moiety. This can be regarded as a captodative effect.

Degradation of the Cu^{II}–phenoxyl radical complex: After one week of aerobic incubation (253 K) of $[Cu^{II}(LOMe)(CH_3CN)]$ with one equivalent of the single-electron chemical oxidant $TPASbCl_6$, an unexpected degradation product was isolated (formation of an transient $[Cu^{II}(LOMe^{\bullet})(CH_3CN)]^{+}$ species was evidenced by EPR and UV/Vis spectroscopy): the copper complex retained its square-pyramidal structure and only modification of the phenolic subunit was observed. The classical oxidative cleavage of the tertiary amine does not occur.[7e] The X-ray structure of $[Cu^{II}_2(LO)_2(Cl)_2]\cdot CH_2Cl_2\cdot Sb_3Cl_{11}$, thus obtained as light green single crystals, shows an *ortho-tert*-butylated quinone moiety in place of the 2-hydroxy-3-*tert*-butyl-5-methoxybenzyl group. The full description of the crystal structure is given in the Supporting Information.

Reactivity of the radical species towards alcohol oxidation: Under anaerobic conditions, addition of an excess of benzyl alcohol to a solution of electrogenerated $[Cu^{II}(LOMe^{\bullet})(CH_3CN)]^{2+}$ or $[Cu^{II}(L{\it t}Bu^{\bullet})(CH_3CN)]^{2+}$ increased the observed rate constant k_{obs} for the comsumption of the radical, while quantitative formation of benzaldehyde (relative to the catalyst) was evidenced by GC. Monoexponential decays were fitted to obtain the pseudo-first-order rate constants k_{obs}. Plots of the observed rate constant $k_{obs}-k_{decay}$ versus benzyl alcohol concentration show a linear dependence (Figure 5) for both complexes. The rate constants k_{ox} for the oxidation of benzyl alcohol obtained from the slopes are $5.8\,M^{-1}min^{-1}$ and $13.6\,M^{-1}min^{-1}$ for $[Cu^{II}(LOMe^{\bullet})(CH_3CN)]^{2+}$ and $[Cu^{II}(L{\it t}Bu^{\bullet})(CH_3CN)]^{2+}$, respectively. One equivalent of benzyl alcohol is oxidized by one equivalent of complex, that is, one mole of the catalyst formally stores two oxidative equivalents: the phenoxyl radical and the Cu^{II} center. A kinetic deuterium isotope effect k^{H}_{ox}/k^{D}_{ox} of 8 was obtained when $PhCH_2OH$ was replaced by $PhCD_2OH$, that is, the rate-limiting step is H abstraction from the substrate, as for GOase and related model compounds.[6b,9] Although $[Cu^{II}(LOMe^{\bullet})(CH_3CN)]^{2+}$

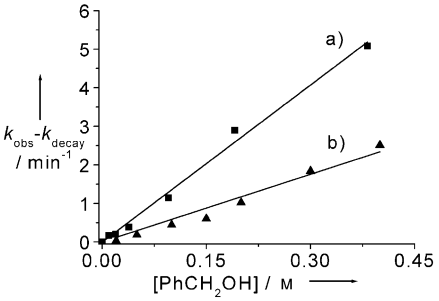

Figure 5. Plot of $k_{obs}-k_{decay}$ versus the concentration of benzyl alcohol: k_{decay} is the rate constant for the radical signal decay in acetonitrile (degradation of the catalyst); the pseudo-first-order constant k_{ox} corresponds to the radical signal decay in presence of an excess of benzyl alcohol; catalysts: $[Cu^{II}(L{\it t}Bu^{\bullet})(CH_3CN)]^{+}$ (a), $[Cu^{II}(LOMe^{\bullet})(CH_3CN)]^{+}$ (b).

Table 4. Spectroscopic and electrochemical properties of copper(II)–phenoxyl complexes in acetonitrile solution.[a]

Complex	λ_{max} [nm](ε [$M^{-1}cm^{-1}$])	EPR	$E_{1/2}$ [V][b]	k_{decay} [min^{-1}]	$t_{1/2}$ [min]
$[Cu^{II}(HL'OMeNO_2^{\bullet})(OAC)]^{+}$	410 (19000)[c]	silent	0.08	1.05	0.66
$[Cu^{II}(L'OMeNO_2^{\bullet})(Pyr)]^{+}$	390 (15300)	$S=1$	−0.08	0.155	5
$[Cu^{II}(L'OMe_2^{\bullet})(Pyr)]^{+}$	425(1000)[d]	$S=1$	−0.16	0.71	1
$[Cu^{II}(LOMe^{\bullet})(CH_3CN)]^{2+}$	426 (5100), 552 (560)	$S=1$	0.02	0.008	87
$[Cu^{II}(LOMe^{\bullet})(Pyr)]^{2+}$	406 (8200)	$S=1$	0.01	0.0045	154
$[Cu^{II}(L{\it t}Bu^{\bullet})(CH_3CN)]^{2+}$	416 (1900), 650 (500)	$S=1$	0.15	0.155	5
$[Cu^{II}(L{\it t}Bu^{\bullet})(Pyr)]^{2+}$	417 (3500), 660 (800)	$S=1$	0.17	0.087	8
active GOase	444 (5200), 800 (3200)	silent	−0.23	–	–

[a] UV/Vis spectra recorded at 233 K, EPR spectra at 100 K. k_{decay} and $t_{1/2}$ at 298 K. [b] Versus Fc/Fc^{+}, 298 K in acetonitrile, 0.1 M TBAP. [c] In CH_3CN/CH_2Cl_2 (50/50). [d] Underestimated due to the low stability of this complex.

and $[Cu^{II}(LtBu^{\bullet})(CH_3CN)]^{2+}$ oxidize benzyl alcohol more slowly than $[Cu^{II}(L'OMeNO_2^{\bullet})]$, the ratio k_{ox}/k_{decay} is higher. It is also 100 times higher than the value reported for a previously described complex.[6b]

$[Cu^{II}(LNO_2^{\bullet})(CH_3CN)]^{2+}$ and $[Cu^{II}(LF^{\bullet})(CH_3CN)]^{2+}$ were not stable enough to study their reactivity at room temperature in the presence of a substrate. Moreover, excess pyridine competitively inhibits substrate binding.

Ethanol was oxidized aerobically to acetaldehyde by the Cu^{II}–phenoxyl radical complex of $[Cu^{II}_2(L'OMe_2)_2]$: 40 ± 5 turnovers were achieved in 30 min at 298 K.[15] On the other hand, $[Cu^{II}(LOMe^{\bullet})(CH_3CN)]^{2+}$ and $[Cu^{II}(LtBu^{\bullet})(CH_3CN)]^{2+}$ oxidized ethanol to acetaldehyde only stoichiometrically, even in the presence of O_2 and a base. However, electrocatalysis in the presence of a catalytic amount of NEt_3 allows 5 ± 1 turnovers to be achieved for the oxidation of ethanol. In constrast to the reduced complexes of N_2O_2 ligands, the Cu^{II}–phenoxyl complexes of N_3O ligands after oxidation of the substrate are not regenerated with O_2. Proton transfer from the substrate to O_2 cannot be achieved efficiently in the absence of a coordinating phenolate. This unambiguously shows that the axial phenol/phenolate in the copper complexes of the N_2O_2 ligands is involved in a protonation–deprotonation process during the catalytic cycle, as in GOase.

Conclusion

The solution chemistry of the copper complexes of N_2O_2 ligands (2 phenol, 1 pyridine group) differs significantly from that of N_3O ligands (1 phenol, 2 pyridine groups): the former afforded stable dimeric structures that can be converted to monomers by addition of a coordinating base, while the latter were isolated only as monomers. The properties of the electrogenerated Cu^{II}–phenoxyl radical species can be finely tuned by changing 1) the number of phenolic arms, 2) the electronic properties of the phenol *p*-substituent and 3) the exogenous ligand. The monomeric copper complexes of the N_2O_2 ligands have lower redox potentials that favor formation of a radical species. The electrochemically generated N_2O_2 Cu^{II}–phenoxyl species are highly reactive and much less stable than their N_3O analogues. All the Cu^{II}–phenoxyl complexes stoichiometrically oxidize benzyl alcohol to benzaldehyde in the absence of O_2 with a rate limiting step that is, as for GOase, H abstraction from the substrate. The reaction proceeds much more slowly when N_3O ligands are used. The aerobic oxidation of ethanol to acetaldehyde by the Cu^{II}–phenoxyl copper complexes of N_3O ligands proceeds stoichiometrically, while 40–80 turnovers are achieved with the N_2O_2 complexes: the acido-basic phenol is needed (and cannot be replaced by acido-basic pyridine) for regeneration of the catalyst.

Formation of a transient phenoxyl radical axially coordinated to the copper atom has been evidenced; it constitutes a model of the GOase active site in its Cu^{II} radical state prior to proton transfer from the coordinated substrate to the axial tyrosyl group according to the theoretical scheme proposed by F. Himo et al.[4a] These results also support the recent proposition that tyrosyl radicals axially coordinated to metal atoms could be of major biological interest in enzymatic catalysis.[16]

Experimental Section

General: All chemicals were of reagent grade and used without purification. NMR spectra were recorded on a Bruker AM 300 (^1H at 300 MHz, ^{13}C at 75 MHz). Chemical shifts are given relative to tetramethylsilane (TMS). Mass spectra were recorded on a Thermofunnigen (EI/DCI) or a Nermag R 101 C (FAB+) apparatus. Microanalyses were performed by the Service Central d'Analyse du CNRS (Lyon, France).

UV/Vis spectroscopy: UV/Vis spectra were recorded on a Perkin Elmer Lambda 2 spectrophotometer equiped with a temperature controller unit set at 298 K. The quartz cell path length was 1.000 cm. Low-temperature Vis spectra were recorded on an UVIKON spectrophotometer equipped with a quartz Dewar (H.S. Martin Inc.) containing a quartz cell of 1.000 cm path length.

Electrochemistry: Electrochemical measurements were carried out using a PAR model 273 potentiostat equipped with a Kipp-Zonen *x*–*y* recorder. Experiments were performed in a standard three-electrode cell under argon atmosphere. An $Ag/AgNO_3$ (0.01M) reference electrode was used. All the potentials given in the text are referred to the regular Fc/Fc^+ redox couple used as an internal reference (+87 mV versus $Ag/AgNO_3$). A vitrous carbon disc electrode (5 mm diameter) was used as working electrode and was polished with 1 μm diamond paste. The electrochemical behaviour of the ligands and complexes was studied by cyclic voltammetry (CV) in acetonitrile solutions containing 0.1M tetrabutylammonium perchlorate (TBAP) as supporting electrolyte. Electrolysis was performed at 233 K using the same apparatus and a carbon-felt working electrode.

EPR spectroscopy: X-band EPR spectra were recorded on a Bruker ESP 300E spectrometer equipped with a Bruker nitrogen flow cryostat, or a Bruker EMX spectrometer equipped with an ESR 900 helium flow cryostat (Oxford Instruments). Samples of the protonated copper complexes of the N_3O ligands were prepared in acetonitrile with a few drops of toluene and CH_2Cl_2 to improve the resolution of the spectrum. Spectra were treated with the WINEPR software and simulated using the Bruker SIMFONIA software.

Crystal structure analysis: For all structures, collected reflections were corrected for Lorentzian and polarization effects but not for absorption. The structures were solved by direct methods and refined with TEXSAN software. All non-hydrogen atoms were refined with anisotropic thermal parameters. Hydrogen atoms were generated in idealized positions, riding on the carrier atoms, with isotropic thermal parameters. CCDC-198361 ($[Cu^{II}_2(L'OMe_2)_2]$), CCDC-199022 ($[Cu^{II}(LtBuH)(CH_3CN)](ClO_4)_2$), CCDC-198776 ($[Cu^{II}(LNO_2)(Cl)]$), CCDC-198520 ($[Cu^{II}(LFH)(CH_3CN)](ClO_4)_2$), CCDC-198701 ($[Cu^{II}(LOMeH)(CH_3CN)](ClO_4)_2$), CCDC-198860 ($[Cu^{II}(LNO_2H)(CH_3CN)](ClO_4)_2$), and CCDC-199566 ($[Cu^{II}_2(LO)_2(Cl)_2]$) contain the supplementary crystallographic data for this paper; these data can be obtained free of charge via http://www.ccdc.cam.ac.uk/conts/retrieving.html.

Oxidation of ethanol: The nonradical N_2O_2 complex was dissolved in ethanol (0.1M, TBAP) to give a 1 mM solution, and one-electron electrochemical oxidation was performed at low temperature (233 K). The base was then added, and the temperature raised to 298 K. The solution was stirred for 30 min at 298 K under ambient O_2 pressure. Prior to analysis, the aliquots were passed through a column containing the ion-exchange resin Dowex 50X2-200. Acetaldehyde was titrated spectrophotometrically by using the 3-methyl-2-benzothiazolone hydrazone test (E. Sawicki, T.R. Hauser, T.W. Stanley, W. Elbert, *Anal. Chem.* **1961**, *33*, 93).

The electrocatalysis experiment was performed with the N_3O catalysts: Electrolysis of the nonradical complex (1 mM in ethanol) was conducted directly in the presence of base at 298 K until a residual current corresponding to 1% of the initial current was obtained. Coulometric titration revealed five exchanged electrons at this time. The aliquots were analyzed in a similar way as described above.

Oxidation of benzyl alcohol: A 2 mM solution of $[Cu^{II}(LtBu)(CH_3CN]^+$ or $[Cu^{II}(LOMe)(CH_3CN]^+$ was electrochemically oxidized at 233 K (CH_3CN, TBAP 0.1M). A 25 μL aliquot was quickly heated to 298 K and diluted in 475 μL of a solution of CH_3CN containing benzyl alcohol (298 K). The disappearance of the 410 nm absorption was monitored by UV/Vis spectroscopy. The yield of benzaldehyde was determined by GC with mesitylene as an internal standard (experimental error 10%).

(2-Hydroxy-3-*tert*-butyl-5-nitrobenzyl)bis(2-pyridylmethyl)amine (LNO_2H): 2-bromomethyl-6-*tert*-butyl-4-nitrophenyl acetate (3.36 g, 10 mmol), prepared according to a described method,[10] bis(2-pyridylmethyl)amine (1.99 g, 10 mmol), NaI (1.5 g, 10 mmol) and Na_2CO_3 (3.18 g, 30 mmol) in THF (90 mL) were stirred for 3 d at room temperature. The solution was filtered and the solvent evaporated. The crude acetate salt was hydrolyzed with sodium hydroxide (25 mL, 40% in water) and ethanol (25 mL). Ethanol was removed and HCl was added to neutralization. The solution was poured into water, and the mixture extracted with CH_2Cl_2. Organic layers were dried (Na_2SO_4) and evaporated. Column chromatography on silica gel (hexane/ethyl acetate 1/1) yielded LNO_2H (4g, 60%) as a white solid; ^{1}H NMR (300 MHz, $CDCl_3$, 298 K, TMS): $\delta = 1.49$ (s, 9H; *t*Bu), 3.38 (s, 2H; H7), 3.91 (s, 4H; H8 and H9), 7.23 (ddd, ^3J(H2,H1) = 4.98 Hz, ^3J(H2,H3) = 7.41 Hz, ^4J(H2,H4) = 1.08 Hz, 1H; H2), 7.28 (d, ^3J(H4,H3) = 7.56 Hz, 1H; H4), 7.64 (ddd, ^3J(H3,H2) = ^3J(H3,H4) = 7.56 Hz, ^4J(H3,H1) = 1.80 Hz, 1H; H3), 7.89 (d, ^4J(H5,H6) = 2.82 Hz, 1H; H5 or H6), 8.14 (d, ^4J(H5,H6) = 2.82 Hz, 1H; H5 or H6), 8.57 ppm (d, ^3J(H1,H2) = 4.98 Hz, 1H; H1); ^{13}C NMR (75 MHz, $CDCl_3$, 298 K, TMS): $\delta = 29.52$ (q), 35.53 (s), 57.16 (t), 59.22 (t), 122.75 (d), 123.18 (d), 123.56 (s), 123.64 (d), 124.64 (d), 137.21 (d), 138.10 (s), 139.43 (s), 149.25 (d), 157.90 (s), 163.65 ppm (s); MS (DCI, NH_3, isobutane): *m*/*z*: 407 (LNO_2H); elemental analysis (%) calcd for $C_{23}H_{26}N_4O_3$: C 67.96, H 6.45, N 13.78; found: C 68.22, H 6.66, N 13.74.

(2-Hydroxy-3-*tert*-butyl-5-fluorobenzyl)bis(2-pyridylmethyl)amine (LFH): 2-*tert*-Butyl-4-fluorophenol (168 mg, 1 mmol), prepared according to Vanholm et al.,[17] bis(2-pyridylmethyl)amine (238 mg, 1.2 mmol) and formaldehyde (375 μL of a 37% aqueous solution) in EtOH/H_2O (4/6, 10 mL) were heated for 24 h at 353 K. The reaction mixture was added to water (50 mL) and extracted with CH_2Cl_2 (2 × 50 mL). The organic layer was dried (Na_2SO_4) and evaporated. The ligand was purified by column chromatography on silica gel with hexane/ethyl acetate (9/1 to 5/5) as eluent. LFH (342 mg, 90%) was obtained as a white solid; ^{1}H NMR (300 MHz, $CDCl_3$, 298 K, TMS): $\delta = 1.43$ (s, 9H; *t*Bu), 3.76 (s, 2H; H7), 3.84 (s, 4H; H8 and H9), 6.58 (dd, ^4J(H5,H6) = 3.10 Hz, ^3J(H5,F) or ^3J(H6,F) = 8.97 Hz, 1H; H5 or H6), 6.90 (dd, ^4J(H5,H6) = 3.10 Hz, ^3J(H5,F) or ^3J(H6,F) = 8.97 Hz, 1H; H5 or H6), 7.14 (ddd, ^3J(H2,H1) = 5.37, ^3J(H2,H3) = 8.31, ^4J(H2,H4) = 0.90 Hz, 1H; H2), 7.32 (d, ^3J(H4,H3) = 8.31 Hz, 1H; H4), 7.61 (ddd, ^3J(H3,H4) = ^3J(H3,H2) = 8.31 Hz, ^4J(H3,H1) = 1.77 Hz, 1H; H3), 8.52 (d, ^3J(H1,H2) = 5.37 Hz, 1H; H1); ^{13}C NMR (75 MHz, $CDCl_3$, 298 K, TMS): $\delta = 29.38$ (q), 35.02 (s), 57.51 (t), 59.25 (t), 112.88 (d), 113.18 (d), 113.58 (d), 113.89 (s), 122.43 (d), 123.61 (d), 136.85 (d), 148.99 (d), 152.31 (s), 152.33 (s), 157.88 ppm (s); ^{19}F NMR (282.54 MHz, $CDCl_3$, 298 K): $\delta = 35.11$ ppm (dd, ^3J(H5,F) = ^3J(H6,F) = 8.8 Hz); MS (DCI, NH_3, isobutane): *m*/*z*: 380 (LFH); elemental analysis (%) calcd for $C_{23}H_{26}FN_3O$: C 72.80, H 6.91, N 11.07, F 5.01; found: C 73.09, H 6.89, N 10.94, F 4.83.

(2-Hydroxy-3,5-di-*tert*-butylbenzyl)bis(2-pyridylmethyl)amine (L*t*BuH): L*t*BuH was synthesized according to the procedure used for LFH using 2,4-di-*tert*-butyl-4-phenol instead of 2-*tert*-butyl-4-fluorophenol. LtBuH was previously described.[6f]

(2-Hydroxy-3-*tert*-butyl-5-methoxybenzyl)bis(2-pyridylmethyl)amine (LOMeH): LOMeH was synthesized according to the procedure used for HLF using 2-*tert*-butyl-4-methoxyphenol instead of 2-*tert*-butyl-4-fluorophenol. LOMeH (1.028 g, 55%) was obtained as a pale orange solid; ^{1}H NMR (300 MHz, $CDCl_3$, 298 K, TMS): $\delta = 1.44$ (s, 9H; *t*Bu), 3.73 (s, 3H; OCH_3), 3.79 (s, 2H; H7), 3.86 (s, 4H; H8 and H9), 6.48 (d, ^4J(H5,H6) = 2.94 Hz, 1H; H5 or H6), 6.80 (d, ^4J(H5,H6) = 3.06 Hz, 1H; H5 or H6), 7.16 (ddd, ^3J(H2,H1) = 4.99 Hz, ^3J(H2,H3) = 7.55 Hz, ^4J(H2,H4) = 1.15 Hz, 1H, H2), 7.34 (d, ^3J(H4,H3) = 7.94 Hz, 1H; H4), 7.61 (ddd, ^3J(H3,H4) = ^3J(H3,H2) = 7.68 Hz, ^4J(H3,H1) = 1.79 Hz, 1H; H3), 8.70 ppm (d, ^3J(H1,H2) = 4.08 Hz, 1H; H1); ^{13}C NMR (75 MHz, $CDCl_3$, 298 K, TMS): $\delta = 29.83$ (q), 35.33 (s), 56.12 (q), 58.47 (t), 112.57 (d), 113.49 (d), 116.71 (s), 122.66 (d), 123.40 (s), 123.99 (d), 137.08 (d), 138.29 (s), 149.33 (d), 150.62 (s), 152.00 (s), 158.39 ppm (s); MS (DCI, NH_3, isobutane): *m*/*z*: 392 (LOMeH); elemental analysis (%) calcd for $C_{24}H_{29}N_3O_2$: C 73.63, H 7.47, N 10.73; found: C 73.65, H 7.64, N 10.74.

$[Cu^{II}_2(L'OMe_2)_2]$: $L'OMe_2H_2$ (200 mg, 0.407 mmol) was treated with two equivalents of NEt_3 in acetonitrile (10 mL) prior to addition of $Cu(ClO_4)_2 \cdot 6H_2O$ (152 mg, 0.407 mmol). After 12 h at 277 K, the dark brown single crystals of $[Cu^{II}_2(L'OMe_2)_2]$ that had formed were collected by filtration. Elemental analysis (%) calcd for $C_{60}H_{76}N_4Cu_2O_8 \cdot 1H_2O$: C 63.98, H 6.98, N 4.97, Cu 11.28; found: C 63.94, H 6.92, N 4.95, Cu 11.20; FAB+ MS: *m*/*z*: 1107 ($[Cu^{II}_2(L'OMe_2)_2]$); UV/Vis (CH_3CN): λ_{max} [nm] (ε [L mol^{-1} cm^{-1}]): 302 (16.7×10^3), 445 (4.3×10^3), 650 (1.6×10^3).

$[Cu^{II}(LNO_2)(CH_3CN)](ClO_4)$: LNO_2H (100 mg, 0.246 mmol) and $Cu(ClO_4)_2 \cdot 6H_2O$ (92 mg, 0.246 mmol) were dissolved in CH_3CN/CH_2Cl_2 (3/1, 18 mL) in the presence of one equivalent of NEt_3. The solution was stirred for 3 h. Dark green hygroscopic microcrystals of $[Cu^{II}(LNO_2)(CH_3CN)](ClO_4)$ were obtained by slow diffusion of diethyl ether into the CH_3CN/CH_2Cl_2 solution. Elemental analysis (%) calcd for $C_{25}H_{28}N_5CuClO_7 \cdot 2H_2O \cdot 0.25CH_2Cl_2$: C 45.48, H 4.91, N 10.50, Cu 9.53; found: C 45.96, H 4.76, N 10.61, Cu 9.54; EPR (9.41 GHz, 100 K, CH_3CN): $g_{xx} = 2.050$, $g_{yy} = 2.074$, $g_{zz} = 2.247$, $A_{xx} = 0.5$ mT, $A_{yy} = 1.5$ mT, $A_{zz} = 17.2$ mT; FAB+ MS: *m*/*z*: 469 ($[Cu^{II}(LNO_2)]$); UV/Vis (CH_3CN): λ_{max} [nm] (ε [L mol^{-1} cm^{-1}]): 390 (11.2×10^3), 517 (6.4×10^3).

$[Cu^{II}(LNO_2H)(CH_3CN)](ClO_4)_2$: LNO_2H (200 mg, 0.492 mmol) and $Cu(ClO_4)_2 \cdot 6H_2O$ (184 mg, 0.492 mmol) were dissolved in acetonitrile (4 mL), and the solution was stirred for one day. Blue microcrystals of $[Cu^{II}(LNO_2H)(CH_3CN)](ClO_4)_2$ were obtained by slow diffusion of toluene into a solution of the complex in CH_3CN/CH_2Cl_2 (3/1). Elemental analysis (%) calcd for $C_{25}H_{29}N_5CuCl_2O_{11}$: C 42.29, H 4.12, N 9.86, Cu 8.95, Cl 9.99; found: C 42.08, H 4.24, N 10.16, Cu 8.91, Cl 10.13; EPR (9.41 GHz, 100 K, CH_3CN): $g_{xx} = 2.066$, $g_{yy} = 2.066$, $g_{zz} = 2.230$, $A_{xx} = 0.5$ mT, $A_{yy} = 1.5$ mT, $A_{zz} = 18.0$ mT; FAB+ MS: *m*/*z*: 470 ($[Cu^{II}(LNO_2H)]$); UV/Vis (CH_3CN): λ_{max} [nm] (ε = [L mol^{-1} cm^{-1}]): 255 (12.8×10^3); 388 (14.8×10^3); 606 (0.09×10^3). Caution: on exposure to air, the blue crystals rapidly decompose to a green powder.

$[Cu^{II}(LtBuH)(CH_3CN)](ClO_4)_2$: L*t*BuH (200 mg, 0.478 mmol) and $Cu(ClO_4)_2 \cdot 6H_2O$ (179 mg, 0.478 mmol) were dissolved in acetonitrile (8 mL) in the presence of one equivalent of NEt_3. The solution was stirred for three days. Blue hygroscopic microcrystals of $[Cu^{II}(LtBuH)(CH_3CN)](ClO_4)_2$ were obtained by slow diffusion of diethyl ether into a solution of the complex in acetonitrile. Elemental analysis (%) calcd for $C_{29}H_{38}N_4Cl_2CuO_9 \cdot 0.5H_2O$: C 47.71, H 5.38, N 7.67, Cu 8.70, Cl 9.71; found: C 47.99, H 5.31, N 7.64, Cu 8.68, Cl 10.01; EPR (9.41 GHz, 100 K, CH_3CN): $g_{xx} = 2.048$, $g_{yy} = 2.079$, $g_{zz} = 2.233$, $A_{xx} = 1$ mT, $A_{yy} = 1$ mT; $A_{zz} = 18.0$ mT; ESI MS: *m*/*z*: 481 ($[Cu^{II}(LtBuH)]$); UV/Vis (CH_3CN): λ_{max} [nm] (ε [L mol^{-1} cm^{-1}]): 600 (0.18×10^3).

$[Cu^{II}(LOMeH)(CH_3CN)](ClO_4)_2$: LOMeH (200 mg, 0.512 mmol) and $Cu(ClO_4)_2 \cdot 6H_2O$ (190 mg, 0.512 mmol) were dissolved in acetonitrile (8 mL) in the presence of one equivalent of NEt_3. The solution was stirred for three days. $[Cu^{II}(LOMeH)(CH_3CN)](ClO_4)_2$ was obtained as blue crystals by slow diffusion of di-*n*-butyl ether into the acetonitrile solution. Elemental analysis (%) calcd for $C_{26}H_{32}N_4CuCl_2O_{10}$: C 44.93, H 4.64, N 8.06, Cu 9.14; found: C 45.05, H 4.61, N 8.14, Cu 8.98; EPR (9.41 GHz, 100 K, CH_3CN): $g_{xx} = 2.066$, $g_{yy} = 2.066$, $g_{zz} = 2.233$, $A_{xx} = 0.5$ mT, $A_{yy} = 1.5$ mT, $A_{zz} = 18$ mT; FAB+ MS: *m*/*z*: 454 ($[Cu^{II}(LOMeH)]$); UV/Vis (CH_3CN): λ_{max} [nm] (ε [L mol^{-1} cm^{-1}]): 400 (0.32×10^3); 590 (0.23×10^3).

$[Cu^{II}(LFH)(CH_3CN)](ClO_4)_2$: LFH (200 mg, 0.528 mmol) and $Cu(ClO_4)_2 \cdot 6H_2O$ (197 mg, 0.528 mmol) were dissolved in CH_3CN/CH_2Cl_2 (3/1, 8 mL) in the presence of one equivalent of NEt_3. The solution was stirred for three days. Blue, hygroscopic microcrystals of $[Cu^{II}(LFH)(CH_3CN)](ClO_4)_2$ were obtained by slow diffusion of diethyl ether (2 mL) into the solution of the complex in acetonitrile. Elemental analysis (%) calcd for $C_{25}H_{29}N_4CuFCl_2O_9 \cdot 0.5H_2O$: C 43.39, H 4.37, N 8.10, Cu 9.18, Cl 10.25; found: C 42.78, H 4.27, N 7.71, Cu 9.07, Cl 10.69; EPR (9.41 GHz, 100 K, CH_3CN): $g_{xx} = 2.064$, $g_{yy} = 2.064$, $g_{zz} = 2.233$, $A_{xx} = 0.5$ mT, $A_{yy} = 1.5$ mT, $A_{zz} = 18.0$ mT; ESI MS: *m*/*z*: 442 ($[Cu^{II}(LFH)]$); UV/Vis (CH_3CN): λ_{max} [nm] (ε [L mol^{-1} cm^{-1}]): 550 (0.24×10^3).

Caution: Perchlorates are potentially explosive and should be handled with special care.

Aknowledgements

The authors thank the Institute of Metals in Biology of Grenoble that provided facilities for performing 4 K EPR, Dr. Stephane Ménage for technical assistance in these experiments and Mylène Vial for the crystallization of $[Cu^{II}_2(L'OMe_2)_2]$.

[1] M. Fontecave, J.-L. Pierre, *C. R. Acad. Sci. Paris Chimie* **2001**, 4, 531.
[2] J. W. Whittaker in *Metal Ions in Biological Systems*, *Vol. 30* (Eds.: H. Sigel, A. Sigel), Marcel Dekker, New York, **1994**, pp. 315–360.
[3] N. Ito, S. E. V. Phillips, K. D. S. Yadav, P. F. Knowles, *J. Mol. Biol.* **1994**, *238*, 794.
[4] a) F. Himo, L. A. Eriksson, F. Maseras, P. E. M. Siegbahn, *J. Am. Chem. Soc.* **2000**, *122*, 8031; b) U. Rothlisberger, P. Carloni, K. Doclo, M. Parrinello, *J. Biol. Inorg. Chem.* **2000**, 5, 236.
[5] a) B. A. Jazdzewski, W. B. Tolman, *Coord. Chem. Rev.* **2000**, *200–202*, 633–685; b) S. Itoh, M. Taki, S. Fukuzumi, *Coord. Chem. Rev.* **2000**, *198*, 3–20; c) Y. Wang, J. L. DuBois, B. Hedman, K. O. Hodgson, T. D. P. Stack, *Science* **1998**, *279*, 537; d) Y. Wang, T. D. P. Stack, *J. Am. Chem. Soc.* **1996**, *118*, 13097; e) P. Chaudhuri, M. Hess, U. Flörke, K. Wieghardt, *Angew. Chem.* **1998**, *110*, 2340; *Angew. Chem. Int. Ed.* **1998**, *37*, 2217; f) P. Chaudhuri, M. Hess, J. Müller, K. Hildenbrandt, E. Bill, T. Weyhermüller, K. Wieghardt, *J. Am. Chem. Soc.* **1999**, *121*, 9599; g) P. Chaudhuri, M. Hess, T. Weyhermüller, K. Wieghardt, *Angew. Chem.* **1999**, *111*, 1165; *Angew. Chem. Int. Ed.* **1999**, *38*, 1095.
[6] a) S. Itoh, S. Takayama, R. Arakawa, A. Furuta, M. Komatsu, Y. Ohshiro, A. Ishida, S. Takamuku, S. Fukuzumi, *Inorg. Chem.* **1997**, 36, 1407; b) S. Itoh, M. Taki, S. Takayama, S. Nagatomo, T. Kitagawa, N. Sakurada, R. Arakawa, S. Fukuzumi, *Angew. Chem.* **1999**, 111, 2944; *Angew. Chem. Int. Ed.* **1999**, 38, 2774; c) S. Itoh, M. Taki, H. Kumei, S. Takayama, S. Nagatomo, T. Kitagawa, N. Sakurada, R. Arakawa, S. Fukuzumi, *Inorg. Chem.* **2000**, *39*, 3708; d) Y. Shimazaki, S. Huth, S. Hirota, O. Yamaushi, *Inorg. Chim. Acta* **2002**, *331*, 168; e) M. Taki, H. Kumei, S. Itoh, S. Fukuzumi, *J. Inorg. Biochem.* **2000**, *78*, 1; f) Y. Shimazaki, S. Huth, S. Hitora, O. Yamaushi, *Bull. Chem. Soc. Jpn.* **2000**, *73*, 1187.
[7] a) M. Taki, H. Kumei, S. Nagatomo, T. Kitagawa, S. Itoh, S. Fukuzumi, *Inorg. Chim. Acta* **2000**, *300–302*, 622–632; b) A. Sokolowski, H. Leutbecher, T. Weyhermüller, R. Schnepf, E. Bothe, E. Bill, P. Hildenbrandt, K. Wieghardt, *J. Biol. Inorg. Chem.* **1997**, *2*, 444; c) C. Ochs, F. E. Hahn, R. Fröhlich, *Eur. J. Inorg. Chem.* **2001**, 2427; d) D. Zurita, I. Gautier-Luneau, S. Ménage, J. L. Pierre, E. Saint-Aman, *J. Biol. Inorg. Chem.* **1997**, *2*, 46; e) Y. Shimazaki, S. Huth, A. Odani, O. Yamauchi, *Angew. Chem.* **2000**, *112*, 1732; *Angew. Chem. Int. Ed.* **2000**, *39*, 1666.
[8] a) U. Rajendran, R. Viswanathan, M. Palaniandavar, M. Lakshminarayanan, *J. Chem. Soc. Dalton Trans.* **1992**, 3563; b) M. Vaidyanathan, M. Palaniandavar, T. Balasubramanian, P. Prabharan, T. P. Muthiah, *Inorg. Chem.* **1998**, *37*, 6418.
[9] F. Thomas, G. Gellon, I. Gautier-Luneau, E. Saint-Aman, J.-L. Pierre, *Angew. Chem.* **2002**, 114, 3173; *Angew. Chem. Int. Ed.* **2002**, 41, 3044.
[10] S. Ménage, G. Gellon, J.-L. Pierre, D. Zurita, E. Saint-Aman, *Bull. Soc. Chim. Fr.* **1997**, *134*, 785.
[11] A. W. Addison, T. N. Rao, J. Reedijk, J. Von Rijn, G. C. Verschoor, *J. Chem. Soc. Dalton Trans.* **1984**, 1349.
[12] The complex $[Cu^{II}(LNO_2)(Cl)]$ was found to be poorly soluble in both acetonitrile and CH_2Cl_2, and this prevented further electrochemical and spectroscopic characterization.
[13] To minimize this phenomenon, the $[Cu^{II}(LF)(Pyr)]^+$ and $[Cu^{II}(LF)(CH_3CN)]^+$ complexes were formed as their triflate salts. The supporting electrolyte was replaced by *N*-lithiotrifluoromethanesulfonimide, and a platinum-grid working electrode was used; in this case electrolysis was possible, but the oxidized species were not stable enough to allow their characterization. Coulometric titration revealed a one-electron process.
[14] a) L. Benisvy, A. J. Blake, D. Collison, E. S. Davies, C. D. Garner, E. J. L. McInnes, J. McMaster, G. Whittaker, C. Wilson, *Chem. Commun.* **2001**, 1824; b) P. Chaudhuri, K. Wieghardt, *Prog. Inorg. Chem.* **2001**, 50, 151.
[15] The catalyst is the monomeric species obtained by cleavage of the dimer $[Cu^{II}_2(L'OMe_2)_2]$ by the coordinating solvent ethanol (evidenced by EPR spectroscopy).
[16] a) A. Ivancich, H. M. Jouve, J. Gaillard, *J. Am. Chem. Soc.* **1996**, *118*, 12852; b) A. Ivancich, H. M. Jouve, B. Sartor, J. Gaillard, *Biochemistry* **1997**, *36*, 9356.
[17] U. S. Vanholm, V. D. Parker, *J. Chem. Soc. Perkin Trans. 1* **1973**, 562.

Received: February 24, 2003 [F4880]